NAVAL POSTGRADUATE SCHOOL

MONTEREY, CALIFORNIA

THESIS

TECHNIQUES FOR THE DETERMINATION OF PARTICLE GROWTH FACTORS IN REAL TIME

by

Coriandre T. Johnson

June 2020

Thesis Advisor: Scott Powell
Co-Advisor: Haflidi Jonsson, NPS Retired

THIS PAGE INTENTIONALLY LEFT BLANK

REPORT DOCUMENTATION PAGE			*Form Approved OMB No. 0704-0188*

1. AGENCY USE ONLY *(Leave blank)*	**2. REPORT DATE** June 2020	**3. REPORT TYPE AND DATES COVERED** Master's thesis

4. TITLE AND SUBTITLE TECHNIQUES FOR THE DETERMINATION OF PARTICLE GROWTH FACTORS IN REAL TIME	**5. FUNDING NUMBERS** TJYNZB
6. AUTHOR(S) Coriandre T. Johnson	
7. PERFORMING ORGANIZATION NAME(S) AND ADDRESS(ES) Naval Postgraduate School Monterey, CA 93943-5000	**8. PERFORMING ORGANIZATION REPORT NUMBER**
9. SPONSORING / MONITORING AGENCY NAME(S) AND ADDRESS(ES) Office of Naval Research, Arlington, VA 22217	**10. SPONSORING / MONITORING AGENCY REPORT NUMBER**

11. SUPPLEMENTARY NOTES The views expressed in this thesis are those of the author and do not reflect the official policy or position of the Department of Defense or the U.S. Government.

12a. DISTRIBUTION / AVAILABILITY STATEMENT Approved for public release. Distribution is unlimited.	**12b. DISTRIBUTION CODE** A

13. ABSTRACT (maximum 200 words)

A technique developed by Snider and Petters in 2008 is used to determine hygroscopic growth factors of aerosol particles. Simultaneous measurements from two optical particle-size spectrometers are used, where one measures the particles in the ambient atmosphere, and the other after drying them out. From 8–26 July 2019, aerosol data was collected west of Boca Chica Airfield, Florida. The Naval Postgraduate School's Aviation Facility Twin Otter aircraft, equipped with a forward scattering spectrometer probe (FSSP), passive cavity aerosol spectrometer probe (PCASP), and an aerosol and precipitation spectrometer (CAPS) was used to measure dry and ambient aerosol particles. Comparisons of particle diameters at different ambient relative humidities (RH) were used to estimate the aerosol growth factors (GF). In general, the calculated GF increased as RH increased. GF values obtained varied wildly and ranged from 0.2 to 12.5 between 27 and 95% RH, but averaged into 5% RH ranges, they ranged from 2.0 to 5.5. Using wind direction as an indication of the source of the aerosol suggests some of the variability may be attributed to the aerosol composition.

14. SUBJECT TERMS atmospheric, aerosol, growth, growth factor, hygroscopy	**15. NUMBER OF PAGES** 47
	16. PRICE CODE

17. SECURITY CLASSIFICATION OF REPORT	**18. SECURITY CLASSIFICATION OF THIS PAGE**	**19. SECURITY CLASSIFICATION OF ABSTRACT**	**20. LIMITATION OF ABSTRACT**
Unclassified	Unclassified	Unclassified	UU

NSN 7540-01-280-5500

Standard Form 298 (Rev. 2-89)
Prescribed by ANSI Std. 239-18

THIS PAGE INTENTIONALLY LEFT BLANK

Approved for public release. Distribution is unlimited.

TECHNIQUES FOR THE DETERMINATION OF PARTICLE GROWTH FACTORS IN REAL TIME

Coriandre T. Johnson
Lieutenant Commander, United States Navy
BA, Thomas A. Edison State University, 2007

Submitted in partial fulfillment of the
requirements for the degree of

MASTER OF SCIENCE IN METEOROLOGY AND PHYSICAL OCEANOGRAPHY

from the

NAVAL POSTGRADUATE SCHOOL
June 2020

Approved by: Scott Powell
Advisor

Haflidi Jonsson
Co-Advisor

Wendell A. Nuss
Chair, Department of Meteorology

THIS PAGE INTENTIONALLY LEFT BLANK

ABSTRACT

A technique developed by Snider and Petters in 2008 is used to determine hygroscopic growth factors of aerosol particles. Simultaneous measurements from two optical particle-size spectrometers are used, where one measures the particles in the ambient atmosphere, and the other after drying them out. From 8–26 July 2019, aerosol data was collected west of Boca Chica Airfield, Florida. The Naval Postgraduate School's Aviation Facility Twin Otter aircraft, equipped with a forward scattering spectrometer probe (FSSP), passive cavity aerosol spectrometer probe (PCASP), and an aerosol and precipitation spectrometer (CAPS) was used to measure dry and ambient aerosol particles. Comparisons of particle diameters at different ambient relative humidities (RH) were used to estimate the aerosol growth factors (GF). In general, the calculated GF increased as RH increased. GF values obtained varied wildly and ranged from 0.2 to 12.5 between 27 and 95% RH, but averaged into 5% RH ranges, they ranged from 2.0 to 5.5. Using wind direction as an indication of the source of the aerosol suggests some of the variability may be attributed to the aerosol composition.

THIS PAGE INTENTIONALLY LEFT BLANK

TABLE OF CONTENTS

THIS PAGE INTENTIONALLY LEFT BLANK

LIST OF FIGURES

THIS PAGE INTENTIONALLY LEFT BLANK

LIST OF TABLES

THIS PAGE INTENTIONALLY LEFT BLANK

LIST OF ACRONYMS AND ABBREVIATIONS

AOD	aerosol optical depth
CAPS	cloud aerosol and precipitation spectrometer
CAS	cloud and aerosol spectrometer
CIP	cloud imaging probe
CIRPAS	Center for Interdisciplinary Remotely-Piloted Aircraft Studies
D_{dry}	dry particles
D_{wet}	wet particles
F-300	model 300 forward scattering spectrometer probe
FSSP	forward scattering spectrometer probe
GF	growth factor
HEL	high-energy-laser
LWC	liquid water content
OPC	optical particle counter
PCASP	passive cavity aerosol spectrometer probe
RH	relative humidity
RI	refractive index
T	temperature
TDMA	tandem differential mobility analyzers

THIS PAGE INTENTIONALLY LEFT BLANK

ACKNOWLEDGMENTS

I would like to thank the people whom, without their support, assistance, and love, this thesis would not have been possible. First, my advisor, Professor Haflidi Jonsson, thank you for your patience and guidance and for helping me to complete truly meaningful work. Second, Professor Scott Powell, you are a wealth of knowledge. Thank you for taking the time to be my second reader. Third, LCDR Benjamin "Brodie" Wells, there is no way that this thesis could have been completed without you. I know that you had challenges of your own during the time of writing this thesis, but you took the time to make sure that I had what I needed and even reached out to me for additional suggestions to make the analysis of this project better. Your selflessness means more to me than I can express in words. And last, but not least, my husband, Stuart, daughters, Jade and Phoenix, and son, Roman: Without you all by my side I would not have had the motivation to put my best efforts forward. Thank you for your encouragement, your love, and your unwavering support throughout this process. I love you forever.

THIS PAGE INTENTIONALLY LEFT BLANK

I. INTRODUCTION

Past in situ measurements of aerosol light scattering conclude that hygroscopic particle growth, chemistry, and optical properties are closely coupled (Jefferson et al. 2017). As aerosols in the ambient environment take up water, their size and chemical composition change as a function of relative humidity (RH); and as they grow, we can visually detect their presence as they scatter and absorb light. This ability for particles to take up water, hygroscopicity, is determined by the ratio of hygroscopic to non-hygroscopic material the particle contains (Zieger et al. 2017). During the equilibrium process, the particle comes to a steady size and composition rapidly, and for the purposes of this study, is considered instantaneous (Boucher et al. 2013).

The diversity of sources of aerosol particles bring about large variations in their size distributions and ways in which they grow. Fine aerosol particles originate almost exclusively from condensation of precursor gases. They have large area-to-volume ratios and are difficult to generate mechanically. Coarse particles occur as the result of interaction of the wind with the Earth's surface. Some are directly ripped off the surface and lofted, others form as a result of wave breaking at the surface of the ocean. Thus, coarse particles emitted into the atmosphere may be sea salt, soil, dust, and vegetation debris. The diameters of aerosol particles range over several orders of magnitude, so many fine particles are smaller than the wavelength of light or other electromagnetic radiation and have negligible effect on the optical properties of the atmosphere, but the coarse particles do. Soluble or hygroscopic fine particles, however, may become coarse when RH rises and ample water vapor is available for particle intake. In addition, when RH decreases, a hydrated particle may reach a solubility limit, the point at which a particle of mixed composition can exist in equilibrium in the surrounding atmosphere (Tang and Munkelwitz 1994). Laboratory studies show that for a mixed hydrated particle, in particular one that contains organic material, the RH value required for equilibrium is less than the value required for a particle that is composed of only a single solute (Martin 2000; Marcolli et al. 2004; Parsons et al. 2004; Snider and Petters 2008).

The hygroscopic growth factor (GF) is a widely used parameter in determining the ambient equilibrium size of aerosol particles. In calculating GF, particles sizes are often measured after the RH in the sampled air has changed due to change in ambient temperature. It is difficult to precisely determine this change in RH, and therefore routine methods of evaluation have resolved to dry the particles completely. In doing so, rendering measurements at an unknown equilibrium level is avoided; and GF is defined as the ratio of the particle diameter in in equilibrium with the RH in the ambient atmosphere to the diameter of the completely dry particle. It is dependent upon the particle's chemical composition, and the contained hygroscopic material's tendency to lower the water saturation vapor pressure above that of an aqueous solution (Zamora et al. 2011). As particle compositions vary wildly in the atmosphere, so may GFs.

Uncertainty of hygroscopic properties, and deficient measurement techniques have hindered previous studies that aimed to accurately quantify GF of aerosols across a wide range of aerosol types and compositions. Some inconclusive examples of previous methods used included 1) humidified nephelometer measurements that tend to lack vertical resolution, 2) tandem differential mobility analyzers (TDMAs) that are typically limited to measuring hygroscopic growth of dry particle diameters up to 0.5μm and become less reliable at RH > 90% (Suda and Petters 2012), and 3) laboratory analyses that are constricted due the laboratory environment. In addition, many previous techniques have not proven time-efficient or cost-effective, as is evident in the Hygroscopic Growth of Submicron and Super-micron Aerosols in the Marine Boundary Layer (Zhang et al. 2014) which spanned three research cruises over a period of four years: TexAQS-GoMACCS (2006), ICEALOT (2008) and CalNex (2010).

However, Snider and Petters (2008) developed a technique to derive the hygroscopic growth factor of dry particles by measuring the size spectra of ambient aerosol particles taken from concurrent measurements obtained by airborne optical particle-size spectrometers. Measurements from the 2001 second Dynamics and Chemistry of Marine Stratocumulus (DYCOMS-II) field study, used a Model 300 Forward Scattering Spectrometer Probe (F-300) to measure particles at ambient RH and a Passive Cavity Aerosol Spectrometer Probe (PCASP) to measure dried particles to RH < 40%. The PCASP

and F300 measurements were analyzed to derive GF for dry particles with diameters between 0.3 and 0.6 μm (Snider and Petters 2008 and Strapp et al. 1992).

The objective of this thesis is to develop a technique for rapid computation of the hygroscopic GF. Hygroscopic growth theory along with techniques developed by Snider and Petters (2008) are used as a basis to evaluate measurements of aerosol data collected in a field experiment in July 2019 in an area west of Boca Chica Airfield, Florida. The measurements were obtained from a Passive Cavity Aerosol Spectrometer Probe (PCASP) and Cloud and Aerosol and Precipitation Spectrometer (CAPS). Sampled marine aerosol data at various altitudes and across a range of relative humidity values were evaluated to derive GF. Wind direction at the time and altitude of sample collection was used as a proxy to indicate the origin, and thus possible variability in composition of the aerosol particles. Based on hygroscopic growth theory, and the data presented in previous studies, two hypotheses are presented:

(1) Ambient aerosol particles will exhibit size-dependent hygroscopic behavior for values of RH > 70%; and

(2) Hygroscopic behavior will vary based on aerosol source region, hence wind direction.

The motivation to develop a technique for rapid computation of aerosol GF is the advance of military high-energy-laser (HEL) weapons. Decades of research and development have gone into the production HEL weapons, but their effectiveness is still adversely affected by aerosol scattering and absorption of the HEL beam. Properties of aerosols are often standardized by calculations that use methods that do not align with current conditions and are useless in evaluation of HEL propagation (Zohuri 2016). Furthermore, under normal environmental conditions, scattering and absorption properties of aerosols can change during the fire-to-engagement timeframe. Over a multi-kilometer range and under normal environmental conditions, about half of the laser power loss can be attributed to aerosol scattering (Nielsen 2009 and Zohuri 2016). The total extinction effects on a laser's beam by aerosols are dependent on aerosol size, shape, and refractive index (RI); and scattering cross sections vary with multiple powers of particle size.

Therefore, significant corrections are needed when evaluating the aerosol effect on extinction from measurements of dried-out aerosols. A simultaneous collection of wet and dry particles for the determination of GF would improve accuracy and efficiency for time-sensitive HEL employment.

II. BACKGROUND

A. A BRIEF HISTORY OF AEROSOL SAMPLING

According to Milton Kerker (1997), laboratory-generated aerosols were first recorded by Leonardo da Vinci (1452-1519) to account for the blue color of the sky. However, is was not until John Tyndall (1869) discovered and documented that a beam of light shone through suspended particles and viewed at an angle against a dark background revealed the presence of particles scattered by the scatter of the light. Tyndall was also the first to propose a connection between the light scattered by an aerosol during the early stages of its formation, and the color of the sky and the polarization of light. Tyndall's work and the theoretical contribution from Rayleigh (1871) ushered in major discoveries for aerosol sciences. Faraday (1857) was the first to describe aerosols and establish techniques to research their optical properties using exploding wires and focused sunlight (Gentry 1995).

Historically, measurements of hygroscopic growth by scattered light have been used to describe the behavior of water uptake and the mixed state of ambient aerosol particles. Many inorganic compounds have been found to be hygroscopic. However, organic compounds and mixed compounds have not been well-characterized, and their behavior is predominantly dependent on the resident organic material. Parameterization of the Köhler equation has often been used to describe the equilibrium size of soluble aerosol components, as determined by the saturation vapor pressure. Junge's (1952) visibility studies showed a direct correlation in the change in visibility with changing relative humidity and was attributed to the hygroscopic growth of aerosol particles. Since then, several techniques have been used to measure aerosol growth. Some measurement techniques account for only a single particle, while others measured properties of an entire population; some vary in measurable size range or chemical properties. Some vary in the amount of time required to collect a sample, and others measured optical hygroscopic growth rather than hygroscopic growth in diameter (Kerker 1997).

Contemporary theory of atmospheric physics aims to quantify the evolution of atmospheric aerosol particle size distributions. Values of number size, surface area, and volume, are constitutional characteristics of atmospheric aerosols. Many different approaches are employed to measure aerosols; particle counters, sizers and hygroscopic analyzers can be used for in-situ measurements, and lidar and satellite instruments for remote sensing techniques. Despite significant progress in aerosol measurement techniques over time, further research is needed to adequately quantify their hygroscopic and optical properties, and their influence on light scattering and absorption.

B. AEROSOL MEASUREMENTS

To accurately measure aerosols, a representative sample of the ambient atmosphere must be obtained. In general, atmospheric particles less than 1.0 μm in diameter travel with the gas that they are suspended in, under normal conditions. Larger particles have greater inertia and tend not to exactly follow the ambient flow. This causes particle losses in sampling ducts where flows are bent before entering instruments. A misalignment between the measuring probe and sampled airstream, as well as mismatch in flow speed at the sample intake also could cause difficulties in sampling systems. On aircraft, RAM heating of air samples is a common problem that adds to sample heating by the measuring instruments themselves. Any heating reduces RH and changes the size of the particle.

In temperature and humidity-controlled laboratory settings, growth factors have been studied in detail for various hygroscopic substances (Sorooshian et al. 2007). In airborne field studies, however, collecting aerosol samples without changing the temperature of the sample when drawing it into the instruments presents a challenge, and correcting for ambient temperature and RH values proves to be difficult. Some attempts have been successfully made of using a battery of nephelometers running at different, controlled, RHs (Hegg et al. 2006 and 2007), or by particle size measurements where the humidity of the sample is controlled. These methods are rather tedious, power and space intensive, and sometime require long averaging times. Hence, a simple method, as suggested here, using routine measurements would be valuable.

C. AEROSOL OPTICAL DEPTH

Photometric measurements of light attenuation by airborne particles is often complementary to the particles' mass concentration and chemical composition in determining the transmissivity of the atmosphere. Such Aerosol Optical Depth (AOD) measurements quantify the aerosol attenuation in the atmosphere. AOD is an integral of the scattering coefficient over a path length, and thus responds similarly to changes in particle size at it responds to RH. AOD measurements, however, are of limited use in HEL operation, as they require a known light source. The sun often serves as source but is hardly ever located at the end of the relevant laser path.

D. ATMOSPHERIC EXTINCTION OF LASER ENERGY

Scattering and absorption of laser energy occurs as the propagating beam travels toward its target. The combined effects of scattering and absorption are incorporated in Beer's Law:

$$A = \epsilon bc \quad \text{and} \quad \frac{I}{I_0} = e^{-\epsilon L}$$

where A is absorbance, ϵ is the molar absorptivity (or extinction coefficient), b is the path length of the sample, and c is the concentration of the compound in solution. I is light intensity as it travels through the aerosol, I_0 is the incident light intensity, and L is the path length of the light through the aerosol.

$$\epsilon = \alpha_m + \alpha_a + \beta_m + \beta_a$$

ϵ is the total extinction coefficient. α represents the absorption coefficients and β represents the scattering coefficients, subscripts m and a are the molecular and aerosol contributions, respectively. Any increase in ∈ results in greater atmospheric attenuation of laser light.

Table 1 is a list of molecular atmospheric constituents (Liou 2002). Although H_2O and CO_2 make up a small percentage of the total atmosphere, they dominate the infrared atmospheric absorption spectrum. For optimal laser performance, it is necessary for the spectral width of the beam to fit within a wavelength window with minimal absorption

features. Molecular scattering is described in terms of Rayleigh scattering. Total extinction effects on light by aerosols are like those of molecules. The extent of the effects is dependent on aerosol size, shape, and RI.

Table 1. List of Molecular Atmospheric Constituents. Adapted from Liou (2002).

Gas Name	Chemical Formula	Percent Volume
Nitrogen	**N2**	**78.08%**
Oxygen	O2	**20.95%**
Water	H2O	**0 to 4%**
Argon	Ar	**0.93%**
Carbon Dioxide	CO2	**0.0360%**
Neon	Ne	**0.0018%**
Helium	He	**0.0005%**
Methane	CH4	**0.00017%**
Hydrogen	H2	**0.00005%**
Nitrous Oxide	N2O	**0.00003%**
Ozone	O3	**0.000004%**

III. METHODS

A. FIELD STUDY

The Naval Postgraduate School's Twin Otter research aircraft, equipped with optical particle counters (OPCs) for measuring the size distribution and concentration of aerosol particles, conducted thirteen research flights from 08–25 July 2019 in the W-174 area west of Boca Chica Air Station, Florida. The research team flew for approximately 5 hours per flight in no specific flight pattern, and data collection altitudes ranged from 40 to 4000 meters. The aircraft also collected ambient data to include temperature (T), relative humidity (RH). Wind speed and direction were deduced from the INS/GPS and gust probe measurements.

B. INSTRUMENTATION

Three OPCs designed for aircraft use were mounted on a pylon beneath the right wing of the aircraft. The instruments included a Forward Scattering Spectrometer Probe (FSSP), Passive Cavity Aerosol Spectrometer Probe (PCASP), Cloud and Aerosol and Precipitation Spectrometer (CAPS). However, only two OPCs, the PCASP and CAPS were used exclusively in this study. The PCASP and CAPS were calibrated prior to each flight. The PCASP was calibrated using polystyrene latex spheres, which has an RI of 1.42, and the CAPS with glass beads and an RI of 1.56. Each probe sized particles by measuring the intensity of light that the particle scattered when passing through a laser beam.

Hallar et al. (2005) provided specification of the helium-neon laser beam within PCASP that was focused to a small diameter at the center of an aerodynamically focused, particle laden air stream. Particles that came into contact with the beam scattered light in all directions. A portion of the scattered light was collected by a mirror within the instrument over angles from ~35° to 135° (Hallar et al. 2005). The intensity of the collected light was measured, digitally logged, and classified into twenty size channels (bins). The size of the particles was resolved from the light scattering intensity based on calibrations using engineered, known size spheres, and applying Mie scattering theory calculations to interpolate between calibration points. Low RH within the PCASP was secured by running

its de-icing heaters to add to normal internal heating by its pump and by compression. The measured diameters of dry particles (D_{dry}) ranged from 0.12 to 3.39 μm.

The CAPS include three instruments (1) a cloud imaging probe (CIP), (2) a cloud and aerosol spectrometer (CAS), and (3) a hotwire liquid water content sensor (Hotwire LWC) (Baumgardner et al. 2001). During this study, the CAS measured ambient particles over a size range of 0.59–85.0 μm. Thus, there is an overlap in the size ranges these two instruments measure. The FSSP on the other hand does not overlap much with the PCASP and was primarily used to compare with the CAS for consistency.

Table 2. CAS, PCASP, and FSSP Particle Size Channel Boundaries and Bin Overlap

CAS			PCASP			FSSP		
Channel	Lower	Upper	Channel	Lower	Upper	Channel	Lower	Upper
1	0.59	0.66	1	0.127	0.138	1	2.39	2.65
2	0.66	0.73	2	0.138	0.149	2	2.65	2.91
3	0.73	0.8	3	0.149	0.16	3	2.91	3.27
4	0.8	0.88	4	0.16	0.174	4	3.27	3.75
5	0.88	0.97	5	0.174	0.194	5	3.75	4.39
6	0.97	1.13	6	0.194	0.21	6	4.39	5.0
7	1.13	1.38	7	0.21	0.232	7	5.0	6.0
8	1.38	1.71	8	0.232	0.253	8	6.0	7.15
9	1.71	2.28	9	0.253	0.286	9	7.15	8.51
10	2.28	3.24	10	0.286	0.335	10	8.51	9.54
11	3.24	5.15	11	0.335	0.383	11	9.54	10.7
12	5.15	9.0	12	0.383	0.552	12	10.7	12.1
13	9.0	12.4	13	0.552	0.639	13	12.1	14.1
14	12.4	17.0	14	0.639	0.727	14	14.1	16.2
15	17.0	22.6	15	0.727	0.901	15	16.2	18.9
16	22.6	30.5	16	0.901	1.139	16	18.9	21.4
17	30.5	40.5	17	1.139	1.5	17	21.4	24.4
18	40.5	51.1	18	1.5	2.06	18	24.4	27.6
19	51.1	67.7	19	2.06	2.75	19	27.6	31.7
20	67.7	85.0	20	2.75	3.39	20	31.7	36.0

CAPS, PCASP, and FSSP Overlap

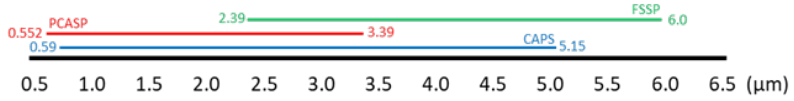

C. DATA ANALYSIS

Of the thirteen flights research flights conducted, twelve captured and recorded aerosol properties that were analyzed and used in hygroscopic growth factor calculations. Data selected for analysis are from cloud-free segments of each flight (legs), which were identified by low values of liquid water content and relative humidity. Cloud-free leg start times were marked by values of RH less than 95% and extended over two-minute intervals unless within the interval RH increased to exceed 95% at any time during the leg. If the cloud-free threshold were exceeded, the algorithm would terminate the leg and advance forward in time, in 20 second intervals, to commence the beginning of the next two-minute leg.

To characterize the aerosol size distributions, number counts of the particles were divided into 20 size bins (Table 2). Each was converted into lognormal distributions, as this conversion generally provides the most appropriate display of aerosol size distributions across several orders of magnitude. The particle number counts (N_i) for each bin were normalized to each bin width as given by:

$$\frac{dN}{d\ log_{10}\ D_p} = \frac{dN}{log_{10}D_{p,u} - log_{10}D_{p,l}}$$

where dN is the lognormal number concentration of particles in the range for a specified channel, and $d\ log_{10}\ D_p$ is the difference in the logarithm of channel widths. $d\ log_{10}\ D_p$ was calculated by subtracting the logarithm of the specified lower limit of the bin ($log_{10}D_{p,l}$) from the logarithm of the upper limit ($log_{10}D_{p,u}$), thus normalizing for each bin width. To obtain normalized concentration values, the concentration was divided by each bin width.

Figure 1 provides an example of log-normal size distributions from samples taken mid-morning on July 14, 2019 and illustrates differences in measured dry particle size distributions as compared to corresponding wet size distributions. In Figure 1a, with a lower RH (50%), all probes agree, as the ambient aerosol is dry, but with higher ambient RH (73%) CAS and FSSP measure larger particles than PCASP (Figure 1b). The assumption that this difference is due to hygroscopic growth of the particles is fundamental

to this analysis. The dry measurements suggest that the probes are in agreeance, and that using such differences to determine GF may be feasible (TSI, 2012).

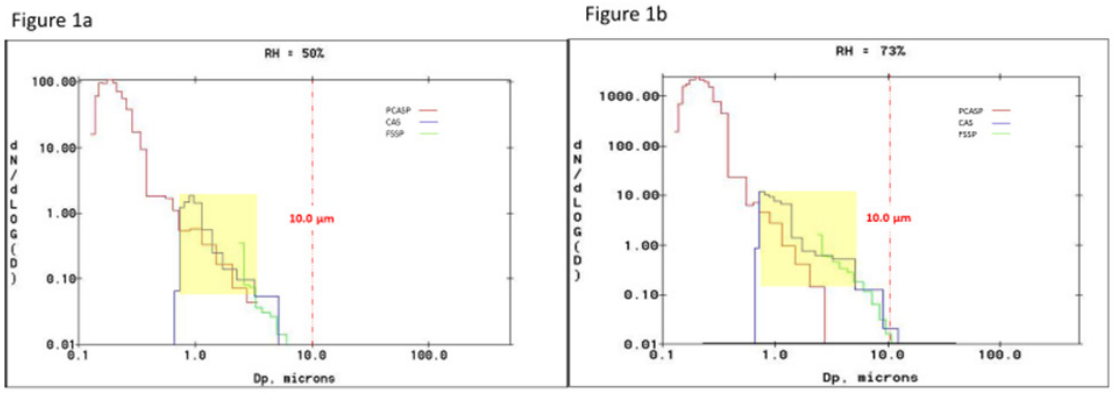

Aerosol number concentration vs. diameter as measured by PCASP (red), CAS (blue), and FSSP (green) for a) RH = 50% and b) RH = 73%. The red dashed line at 10.0 µm illustrates the larger particle diameter with increased RH measured by CAS and FSSP.

Figure 1. Aerosol Number Concentration vs. Diameter

D. GROWTH FACTOR

A comparison of normalized particle concentrations over the range of averaged diameters for dry and wet particles was assessed, and the upper and lower bounds considered for GF calculation were selected based on the range of particle concentration and diameter overlap of PCASP and CAS. For the cases shown in Figures 1a and 1b, the overlap in normalized size distributions and diameters are bounded by the yellow shaded boxes. This defines the subsample of the data used in GF calculations. Hygroscopic growth of aerosol particles was determined by the ratio of the mean diameter of wet aerosols measured by CAS to the mean diameter of dry aerosols measured by PCASP in the overlapping range. Measurements from both instruments were obtained simultaneously. Located on the same pylon, the PCASP and the CAS were approximately two feet apart. The sampled aerosol particles evaluated for GF calculation measured from 0.68 µm to 22.9 µm. Following hygroscopic growth factor theory, the ratio of mean dry particle diameters to mean wet particle diameters at corresponding ambient RH values, provided the hygroscopic growth factor (GF), is

$$GF_{RH} = \frac{D_{wet,\ RH}}{D_{dry,\ RH}}$$

where D_{wet}, RH is the geometric average diameter of the measured diameters of hydrated particles at the specified value of ambient relative humidity and D_{dry}, RH is the geometric average diameter of the measured diameters of a closely co-located dried particles sampled at the same value of RH.

E. AEROSOL COMPOSITION

Determination of an individual ambient aerosol's chemical composition is a complex process and is also a major determining factor in determination of the particle's GF. Organic aerosols can contain hundreds of compounds covering a wide range of chemical and thermodynamic properties (Saxena and Hildemann 1996). Particles may contain different mass fractions of the same compound or varying mass fractions of several. Precise aerosol composition measurements may be done with aerosol mass spectrometers, by collecting particles in a liquid for subsequent laboratory analysis. No such chemical analysis was conducted in this study. Prospero (1999) conducted analysis of aerosol composition at subtropical North Atlantic sites during summer months and correlated wind regimes with dominant aerosol constituents. Following Prospero's evaluation method of aerosol composition, wind direction and speed were used to check for any relation between GF and places where the aerosols may have originated or passed through.

IV. RESULTS

A total of 1,535 legs from twelve research flights encompassing an average of two minutes per leg were studied. Of the total, 1,416 met the threshold criteria of being within the limits of particle concentration and diameter overlap of both instruments with RH values less than 95%. 73% of the calculations were for measurements collected at RH values between 65% and 85%. The sampled aerosol measurements suitable for analysis ranged in diameter from 0.68 μm to 3.05 μm from PCASP, and 0.7 μm to 22.97 μm from CAS.

The calculated hygroscopic growth factors ranged from 0.2 to 12.5, where the largest values were clearly erroneous. Over the entire range of evaluated particles, those with a mean $D_d < 1$ μm and $D_d > 3$ μm represented less than 1% of the sampled population, 1 μm $< D_d <$ 2 μm comprised approximately 26%, and 2 μm $< D_d <$ 3 μm represented about 72%.

Figure 2 shows a preliminary review of Pearson's statistics generated for aerosol and atmospheric parameters at values of RH > 70%. The Pearson's statistics reveal a strong positive correlation (1.0) between the mean numbers of wet and dry particles, a lesser positive correlation (0.75) between the diameters of dry and wet particles and mean wet diameters and growth factors. The mean NovAtel (GPS) altitude shows a strong negative correlation with the mean ambient temperature, as expected. The correlation coefficient between the calculated growth factor and relative humidity is between 0.25 and 0.50.

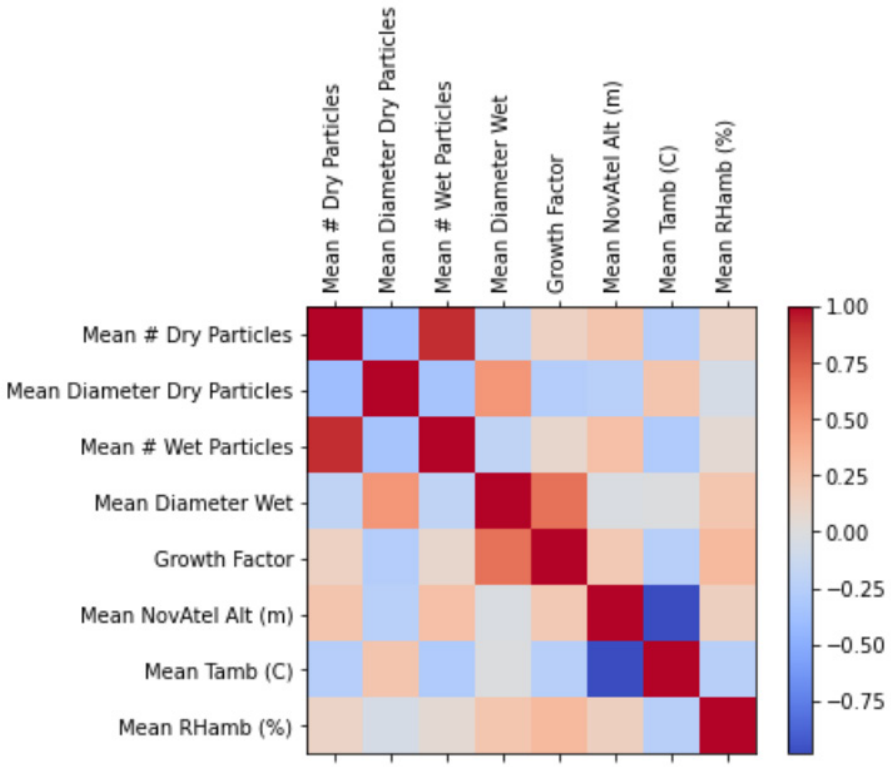

Correlation coefficients between various quantities measured by the aircraft.

Figure 2. Pearson's Correlation Coefficients

Figure 3 shows the calculated growth factors as a function of RH. Color is used to indicate the in-situ wind direction deduced from simultaneous measurements on the aircraft. Immediately apparent is a large scatter in the data, with distribution toward larger GF with increasing RH. The relationship between GF and RH appears to be exponential rather than linear. Also apparent is a nearly asymptotic value of about 2 for relative humidity lower than 60%, above which the spread in scatter in GF increases with RH to factors of 5 to 6.

Figure 3 also indicates that, in general, two different wind regimes dominated the study area during the experiment, with either southeasterly flow (blue points), or southwesterly (yellow) flow. It appears that in the southwesterly winds the aerosol particles were less prone to growth as a function of RH as in the southeasterly flow. For example,

at RH of 70–75%, the median GF in southeasterly and southwesterly winds was, respectively, 2.5 and 1.6.

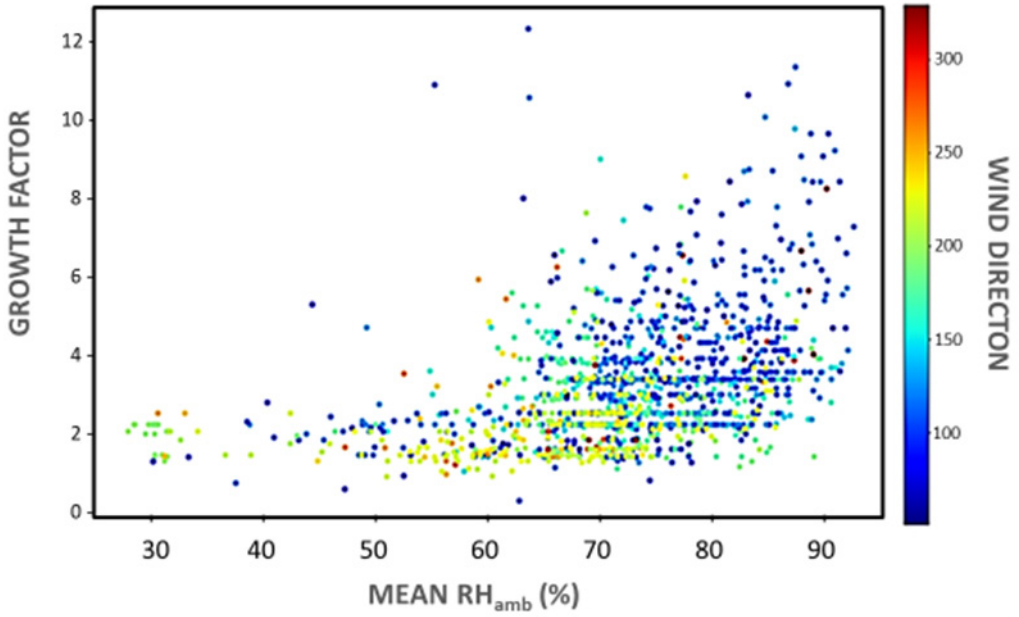

The x-axis is mean ambient relative humidity, y-axis is growth factor. Wind direction is represented by color.

Figure 3. Ambient Relative Humidity vs. Growth Factor

The GF values were averaged over increments of 5% RH (which roughly corresponds to the accuracy of the RH values) and fitted with an exponential function. The resultant fit equation and R^2 values were $GF = 0.79e^{0.025*RH}$ and $R^2 = 0.96$, respectively (Figure 4). Averaged GF values ranged from 1.90 to 5.55 for mean RH between 27 and 95%. Combined, measurements of GF calculations corresponding to 30% < RH < 65% represented only 16 percent of the total sample population, and averages over five percent increments of RH were conducted for fewer than ten samples in some of the lower RH increments. In contrast, the combined number of measurements averaged for 65% < RH < 85% made up 73 percent of the total population. Of note, GF measurements for 70% < RH < 75% accounted for 25 percent of the total population, 352 samples were included within this RH range.

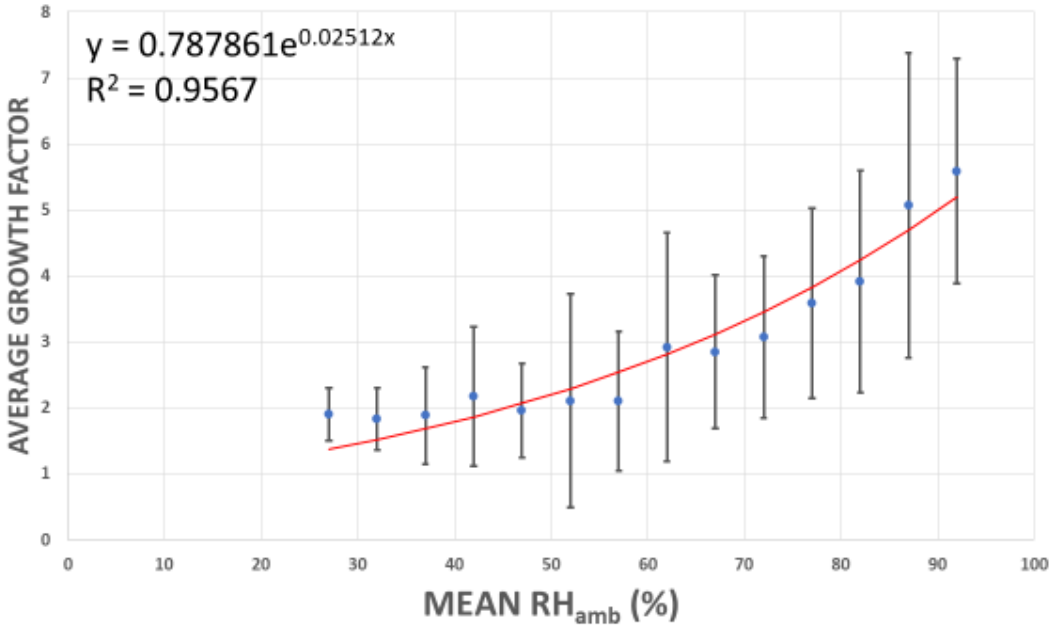

Figure 4. Average Growth Factor vs. Ambient Relative Humidity

A. EVALUATION OF MEASUREMENT ERRORS AND BIASES

To investigate the possibility of error in sizing between PCASP and CAS measurements, aerosol size distribution from both instruments was compared. Together, the instruments were capable of measuring particles from 0.12 µm to 85.0 µm. Table 2 gives the inversion table based on calibrations for both instruments. A comparison of mean diameter measurements and the mean particle concentration for the overlapping diameters between 1.0 µm to 3.0 µm of PCASP and CAS (Figure 1) showed reasonable overlap for all flights.

Biases in GF arise from uncertainty in the RI of particles and phase description are known to cause discrepancies between the "sphere-equivalent dry diameter (D_{dry}) or sphere-equivalent wet diameter (D_{wet})" (Snider and Petters 2008). In practice, the equivalent particle diameter is dependent on its physical property, meaning "the diameter of the sphere that would have the same value as that of the aspherical particle" (Hinds 1999). Atmospheric particle measurements imply that the aerosol particles are spherical. However, the shapes of particles in the atmosphere vary widely. Because the actual

measured particle diameters are not spherical, resultant optical diameter measurements can be over- or under-estimated.

Three points were highlighted from the DYCOMS-II experiment and subsequent evaluation; 1) there is a residence time in PCASP prior to measurement in which the particles are heated and dried, 2) at relatively low values of RH (~ 40%) water content significantly contributed to particle size, and 3) the RI particles at lower RH values varied substantially from the PCASP calibration index (Snider and Petters 2008).

Regarding the residence time in PCASP: The waist of the laser where the particle beam shoots through it is about 100 μm. The pulse width generated by a particle shooting through the laser is on the order of 10 μs. So, the particles have speed of about 10 ms^{-1} going through the laser. The sampling tube is around 10^{-2} m long, so the residence time is on the order of 1 ms. In our measurements, which were synchronized to 1 second, this is insignificant.

Regarding the drying-out of particles in PCASP: Internal heating, mainly generated by a pump internal to the instrument, raises the temperature in the measurement cavity by 10–20°C beyond the ambient. This alone suffices to reduce the RH of the sampled aerosol in most conditions to near zero. In our experiment, to ascertain complete drying of the particle additional heating was provided by operating de-icing heaters at the sample intake. Thus, the only possibility of water remaining on particles is in precipitation where the equilibration process (evaporation rate) may not be fast enough. No precipitation cases are included in this analysis, and even cloud encounters are avoided.

Shapes of particles in the atmosphere may vary widely. Because the actual measured particle diameters are not spherical, like the calibration particles, resultant PCASP diameter measurements may be over- or under-estimated. However, this potential error is minimized by use of optical techniques employing Mangin mirrors to collect light scattered by the particles through 90° of its phase function. This has the effect of smoothing out narrow face-angle effects due to shape as well as Mie resonances.

Soluble particles sized by the CAS are not pure water droplets, but solutions having solute concentration depending on the amount of water taken up. The shape quickly

becomes spherical as deliquescence commences. Solute concentration in the droplet affects the RI. For such mixed particles, which is the likely case for the research environment, it is expected that on account of RI the sphere-equivalent diameter based on the assumption of particle being pure water, may be slightly underestimated.

Following Mie theory, scattering intensities by aerosol particles oscillate between 0.1 μm < Dp < 1.0 μm, which is in the region of instrument overlap. For wavelengths in this range, the PCASP geometry with collection angle from 35° to 135° from forward is less sensitive to the fluctuating scattering intensities than the CAS geometry with about 10° collection angle from 2° to 10° in the forward direction (Strawa et al. 2005). The estimated uncertainty in the sizing accuracy the CAS is ± 30% for particles larger than 1 mm (Strawa et al. 2005). In only two samples analyzed, were diameters from CAS less than 1 μm. The estimated uncertainty of the PCASP is ± 20% for sizing and ± 16% for concentration measurements (Jonsson 1995 and Strawa et al. 2005). The PCASP measured particle sizes are based on an RI of 1.42.

Hallar et al. (2005) states, "The ambiguity in particle concentration in CAS is mainly due to ambiguity in the size of the laser active area, along with the aircraft true airspeed" and that "hese two factors determine the probe's viewing volume." The laser area is a hardware determined value, provided by the instrument manufacturer. Table 3 provides the range of error in average particle size and number concentration for PCASP and CAS for RH values between 70% and 75%, and 80% and 85%. The average dry particle size for RH values between 70% and 75% was 2.30 μm. Given the estimated sizing uncertainty in PCASP of ±20% (Jonsson 1995 and Strawa et al. 2005), the expected diameter range of dry particles should be between 1.84 μm and 2.76 μm. At RH values between 80% and 85%, the average dry particle size was 2.16 μm, and the estimated sizing uncertainty in PCASP should be between 1.73 μm and 2.59 μm. In addition, the error in PCASP concentration measurements was ±16% (Jonsson 1995 and Strawa et al. 2005). The PCASP averaged particle concentration at RH values of 70% to 75% was 17.89; factoring in the expected error, the dry particle concentration could have ranged from 15.03 to 20.75. At 80% to 85% RH, averaged dry particle concentration was 42.74, with the ±16% error we expect that the dry particle concentration ranged from 35.90 to 49.58. The estimated sizing

uncertainty in the CAS was ± 30% for Dp < 1.0 µm (Strawa et al. 2005). At 70% to 75% RH the averaged ambient particle size was 6.49 µm and is expected to range from 5.19 µm to 7.79 µm. At RH values between 80% and 85%, the average ambient particle size was 7.68 µm, and the estimated sizing uncertainty in CAS should be between 6.11 µm and 9.22 µm. Since CAS measured particles at near-ambient conditions, averaged particle concentration measurements at the evaluated RH values did not require correction; averaged particle concentration for RH values between 70% and 75% was 19.36, and 48.99 between 80% and 85% RH.

The GF calculated from averaged particle sizes for RH values between 70% and 75% at the lower ranges of the CAS (5.19 µm) and PCASP (1.84 µm), and higher ranges of CAS (7.79 µm) and PCASP (2.76 µm) were both 2.82; and at RHs between 80% and 85% the lower ranges of the CAS (6.11 µm) and PCASP (1.73 µm), and higher ranges of CAS (9.22 µm) and PCASP (2.59 µm) were 3.53 and 3.56, respectively. Compared to the averaged GFs of 2.91 between 70% and 75% and 3.67 at RH between 80% and 85%. When considering the estimated error for both instruments, the lower and upper bounds of GFs were within 3% of the GF averages without factoring in instrument error. When accounting for the error in PCASP average particle concentrations at RH values between 70% and 75% and 80% and 85% (Table 3), a comparison with particle concentrations from CAS measurements at the same RH values confirms an overlap in particle concentration values.

Table 3. Average Particle Size and Concentration Error Range

	Average Particle Size (µm)						**Avg Particle Concentration**					
	RH_{amb} 70-75%	PCASP Error -20% CAS -30%	PCASP Error +20% CAS +30%	RH_{amb} 80-85%	PCASP Error -20% CAS -30%	PCASP Error +30% CAS +30%	RH_{amb} 70-75%	Avg -16% Error	Avg +16% Error	RH_{amb} 80-85%	Avg -16% Error	Avg +16% Error
PCASP	2.30	1.84	2.76	2.16	1.73	2.59	19.63	16.49	22.77	38.72	32.52	44.95
CAS	6.49	5.19	7.79	7.68	6.11	9.22	20.96	-	-	39.19	-	-

B. DISCUSSION AND CONCLUSION

The large scatter in GFs, especially at GF > 60% (see Figure 3), might be attributed to differences in aerosol chemical composition. The upper bound of GF values is consistent with laboratory results obtained for pure sodium chloride (Sorooshian et al. 2006). Lower GF values scattered below the upper bound envelope may be due to plumes of particles composed of materials other than sea salt, or internal mixtures where particles have complex compositions. Figure 3 shows that in southwesterly winds, i.e., when air was coming from the direction of Cuba, less growth was generally observed than when winds were southeasterly. Although the southeasterly trades may be expected to be more heavily laden with sea-salt, they may be influenced by sources on island in the Caribbean, and sometimes may carry desert dust from Africa. Of note, a Naval training exercise took place in the vicinity of the study site. While taking measurements, multiple ships sailed directly below, and aircraft crossed into the research area numerous times. It is reasonable to assert that exhaust plumes from the ships and airplanes also contributed to the overall aerosol composition. All this would result in variability in GF values, such as we see in Figure 3.

The research aircraft flew into and out of cumulus clouds while collecting air samples. As a result of the cloud-free screening criteria of RH < 95%, some measurements may have been taken in cloud halos near cloud edges, where the chilled mirror instrument used to measure dew point may have been to slow to accurately recording rapid changes, causing erroneous RH values. The RH is calculated from temperature and dew point measurements. Each has an accuracy of about 0.25°C, which translates into about 5% RH (thus the 5% averaging in Figure 4).

The size spectrometers have significant uncertainties. PCASP sizes were retrieved for assumed refractive index of 1.42 based on calibrations. The size of ambient particles having an index of refraction different from the assumed refractive index will be either under- or over-estimated. The theoretical refractive index envelope for the variety of atmospheric aerosol particles in the PCASP response is about 20%. However, the 20 second averaging time used in this study may narrow this error if the actual particle RI fluctuates around that of the calibration aerosol.

Similar issues affect the CAS probe, but in addition and more significantly, its optics are open to the environment and subject to contamination, which affects the measured scattered light pulse heights. This causes shifts the entire response curve of the instrument and causes underestimation of all particle sizes. The view volume of CAS is another possible source of error. The view volume is based on the laser dimensions in the viewing area, and on the accuracy of measurement of true airspeed through the sampling area. The latter is assumed to be equal to the true airspeed of the aircraft, and may differ in turns, climbs, and descent where significant deviation on flow angles from those in straight and level flights occur. The view volume errors have been subject of much attention over the years and remain largely unresolved. Confidence, however, may be established in the applied view volume values by comparing overlapping measurements from other techniques where view volume is determined by relevant measurements, such as PCASP. Figure 1 shows that in dry conditions, where close agreement would be expected, the agreement between these instruments is indeed good.

In laboratory studies deliquescence of aerosol particles occurs abruptly at a certain RH (different for different materials, but typically around RH of ~70%). At RH below deliquescence GF is near zero. However, results of this study show GF values of about 2 at values of RH well below the deliquescence point for most soluble atmospheric aerosols. This could be due to a systematic bias in the size measurements; or it could be due to view volume error in CAS, but we do see it in dry air well above cloud tops, i.e., well above the local marine boundary layer, GFs go to near zero. This suggests that rather than being a measurement artifact, this is the result of hysteresis. Particles that have been through wetting at RH above the deliquescence point, do not dry out again at that point when encountering lower RH again. Instead, they remain in solution, wet, and therefore larger than dry, often to RH of about 20%.

So, although with significant uncertainty in accuracy, it seems the technique of using simultaneous PCASP and CAS measurements to estimate aerosol particle growth factors is practical. This technique may be developed to complement nephelometer measurements to extrapolate scatter measurements of dried air samples to electromagnetic attenuation in the ambient.

THIS PAGE INTENTIONALLY LEFT BLANK

LIST OF REFERENCES

Baumgardner, D., H. Jonsson, W. Dawson, D. O'Conner, *and R* Newton*, 2001,* Oct.: The cloud, aerosol and precipitation spectrometer: a new instrument for cloud investigations, *Atmos. Res.*, **59**–**60**, 251 – 264.

Boucher, O. and Coauthors, 2013: Clouds and aerosols, *Climate Change 2013: The Physical Science Basis*. *Contribution of Working Group I to the Fifth Assessment Report of the IPCC*, *Cambridge University Press*, 571–657, https://doi.org/10.1017/CBO9781107415324.016.

Brechtel, F. J., 2004, Jan.: A versatile droplet sizing spectrometer for aerosol hygroscopic growth measurements from research aircraft, Office of Naval Research, Ser. Number 0001AD, BMI Rep. Number ONR-0004.

Gentry, J. W., 1995, Mar.: The aerosol science contributions of Michael Faraday*, J. of Aerosol Sci.*, **26**, 341–349, https://doi.org/10.1016/0021-8502(94)00110-K.

Hallar, A. et al., 2006, Mar.: Atmospheric radiation measurements aerosol intensive operating period: comparison of aerosol scattering during coordinated flight, *J. of Geophys. Res. Atmos.*, **11**, 5, https://doi.org/10.1029/2005JD006250.

Hegg, D. A., D. S. Covert, K. K. Crahan, H. H. Jonsson, and Y. Liu, Y. 2006, Nov.: Measurements of aerosol size-resolved hygroscopicity at sub- and super-micron sizes, *Geophys. Res*, **Lett. 33**, https://doi.org/10.1029/2006GL026747.

Hegg, D. A., D. S Covert, H. H. Jonsson, and P. A. Covert, 2007, Dec.: An instrument for measuring size-resolved aerosol hygroscopicity at both sub- and super-micron sizes, Aerosol *Sci. Tech,* **41**, 873–883.

Hinds, W. C., 1999: *Aerosol technology: Properties, behavior, and measurement of airborne particles*, 2nd edition, New York: Wiley. Sec 1.2.

Jefferson, A., D. Hageman, H. Morrow, F. Mei, and T. Watson, 2017, Aug.: Seven years of aerosol scattering hygroscopic growth measurements from SGP: factors influencing water uptake, *J. of Geophys. Res. Atmos*, **122**, 17, 9451–9466, https://doi.org/10.1002/2017JD026804.

Jonsson, H. H. et al., 1995, Feb.: Performance of a focused cavity aerosol spectrometer for measurements in the stratosphere of particle size in the 0.06 –2.0 mm diameter range, *J. Atmos. Oceanic Technol*., **12**, 1, 115–129.

Kerker, M., 1997, Apr.: Light scattering instrumentation for aerosol studies: a historical overview, *Aerosol Sci.and Technol*., **27**, 522–540, https://doi.org/10.1080/02786829708965492.

Liou, K. N. 2002: *An introduction to atmospheric radiation*, 2nd ed. San Diego, CA: Academic Press.

Marcolli, C., B. Luo, and T. Peter, 2004, Mar.: Mixing of the organic aerosol fractions: Liquids as the thermodynamically stable phases, *J. Phys. Chem. A.,* **108**, 12, 2216–2224.

Martin, S. T., 2000, Aug.: Phase transitions of aqueous atmospheric particles, *Chem. Rev.*, **100**, 9, 3403–3453.

Orr, C., F. Hurd, and W. J. Corbett, 1958, Oct.: Aerosol size and relative humidity, *J. Coll. Sci. Imp. U. Tok*., **13**, 472–482.

Parsons, M. T., D. A. Knopf, and A. K. Bertram, 2004, Dec.: Deliquescence and crystallization of ammonium sulfate particles internally mixed with water-soluble organic compounds, *J. Phys. Chem. A.*, **108**, 52, 11600–11608.

Prospero, J. M., 1999, Jul.: long-term measurements of the transport of African mineral dust to the southeastern United States: Implications for regional air quality, *J. of Geoph. Res.*, **104**, D13, 15917-15927.

Pruppacher, H. R. and J. D. Klett, 1997: Microphysics of clouds and precipitation, *Kluwer Academic Publ.*, Dordrecht, the Netherlands, 2nd edn.

Saxena, P. and L. Hildemann, 1996, May: Water-soluble organics in atmospheric particles: A critical review of the literature and application of thermodynamics to identify candidate compounds, *J. of Atmos. Chem.,* **24**, 57–109, https://doi.org/10.1007/BF0005382.

Snider, J.R. and M.D. Petters, 2008, Apr.: Optical particle counter measurement of marine aerosol hygroscopic growth, *Atmos. Chem. Phys*., 8, 1949–1962, https://doi.org/10.5194/acp-8-1949-2008.

Sorooshian, A., N. L. Ng, A. W. Chan, G. Feingold, R. C. Flagan, and J. H. Seinfeld, 2007, Jul.: Particulate organic acids and overall water-soluble aerosol composition measurements from the 2006 Gulf of Mexico atmospheric composition and climate study (GoMACCS), *J. Geophys. Res.,* **112**, D13201, https://doi.org/10.1029/2007JD008537.

Strawa, A., R. et al., 2006, Mar.: Comparison of in situ aerosol extinction and scattering coefficient measurements made during the Aerosol Intensive Operating Period, *J. of Geophys. Res.,* **111**, D05S03, https://doi.org/10.1029/2005JD006056.

Tang, I. and H. Munkelwitz, 1994, Sep.: Water activities, densities, and refractive-indicies of aqueous sulfates and sodium-nitrate droplets of atmospheric importance, *J. Geophys. Res.,* **99**, D9, 18801–18808.

TSI Incorperated, 2012: Aerosol statistics lognormal distributions and $DN/d\log D_p$, Application note PR-001 Rev. B, https://www.tsi.com/getmedia/1621329b-f410-4dce-992b-21e1584481a/PR-001-RevA_Aerosol-Statistics-AppNote?ext=.pdf.

Yu, Y. L., C. S. Zhao, Y. Kuang, J. C. Tao, G. Zhao, C. Y. Shen, W. Y. Xu, 2018, Oct.: A parameterization for the light scattering enhancement factor with aerosol chemical compositions, *Atmos. Environ.,* **191**, 370–377, https://doi.org/10.1016/j.atmosenv.2018.08.016.

Zamora, I., A. Tabazadeh, D. Golden, and M. Jacobson, 2011, Dec.: Hygroscopic growth of common organic aerosol solutes, including humic substances, as derived from water, activity measurement. J. of Geophys.l Res., **116**, D23, https://doi.org/10.1029/2011JD016067.

Zieger, P. et al., 2017, Jul.: Revising the hygroscopicity of inorganic sea salt particles. *Nature Communications*, **8**, 15883, https://doi.org/10.1038/ncomms15883.

Zohuri, B., 2016, Aug.: Atmospheric propagation of high-energy laser beams, *Directed Energy Weapons*, 379–414, Cham Springer, https://doi.org/10.1007/978-3-319-31289-7_8.

THIS PAGE INTENTIONALLY LEFT BLANK

INITIAL DISTRIBUTION LIST

1. Defense Technical Information Center
   Ft. Belvoir, Virginia

2. Dudley Knox Library
   Naval Postgraduate School
   Monterey, California